A fourth-order PDE denoising model with an adaptive relaxation method

X. Y. Liu, C.-H. Lai, K. A. Pericleous

School of Computing and Mathematical Sciences, University of Greenwich, UK

X.Liu@gre.ac.uk

Abstract: In this paper, an adaptive relaxation method and a discontinuity treatment of edges are proposed to improve the digital image denoising process by using the fourth-order partial differential equation (known as the YK model) first proposed by You and Kaveh. Since the YK model would generate some speckles into the denoised image, a relaxation method is incorporated into the model to reduce the formation of isolated speckles. An additional improvement is employed to handle the discontinuity on the edges of the image. In order to stop the iteration automatically, a control of the iteration is integrated into the denoising process. Numerical results demonstrate that such modifications not only make the denoised image look more natural, but also achieve a higher value of PSNR.

Keywords: *Image denoising, fourth-order PDE, relaxation method.*

1. Introduction

Image denosing, as one of the most important steps in image preprocesing, has drawn much research interest (see References [1]-[10] and the citations therein). Many researchers proposed a large number of methods to deal with the denoising problem. One of the most successful methods up to now is the BM3D model proposed in [9]. This model adopts a so-called block matching technique and provides a collaborative Wiener filtering to achieve excellent denosisng effect, However, this method requires prior information of the noisy image, i.e., the stand deviation of the noise, which is usually unknown when performing denoising tasks. Amongst many image denoising methods, the use of partial differential equations (PDEs) plays a significant role in the process due to its high efficiency wtihout any prior knowledge. In the literature, various models that make use of different PDEs were proposed, such as the isotropic model [11], the anisotropic model [12] and the total variational model ([8], [9]). These models are based on second order PDEs. A more comprehensive list of relevant scond order models can be found in [15]. One major weakness of using a second order PDE is the generation of a “block effect” [16] in the image. In order to overcome this weakness, You and Kaveh [17] utilized the Laplacian operator, instead of the gradient, of image intensity to establish a fourth order PDE which attracted much

attention. Since then fourth order PDEs are widely used for image denoising ([12]-[15]) and other tasks of image processing ([16], [17]). Some recent methods include the fourth order dual method proposed by Chan[24], the fractional order anisotropic diffusion in [25] and others ([26]-[29]). Apart from the above, some research using high-order PDEs for image processing was carried out in ([30]-[32]). Due to its complex numerical implementation and enormous computation, it has not been very widely used in real applications.

Although the model proposed by You and Kaveh had a significant success in image processing, it has its intrinsic problems. On one hand, it would bring in isolated white and black speckles to the denoised image. On the other hand, the method does not involve an automatic stopping device in the iteration process and thus users have to choose a maximum number of iterations empirically. Therefore the quality of the denoising cannot be fully controlled. In essence, different numbers of iterations may lead to different results. Consequently, developing a proper control of iterations is a useful and crucial way to achieve an automatic denoising process.

In this paper, in order to address the problems of the YK model, an adaptive relaxation method is introduced to relieve the effect of isolated speckles and a discontinuity treatment of edges is adopted to sharpen the discontinuity on the edges of an image. Additionally, a control of the iterative process is employed in the numerical experiments to make the denoising process automatic. With these modifications, the result is superior to that obtained by the YK model.

This paper is organized as follows. In Sect. 2, the YK model is investigated and the reasons for isolated speckles are analysed. As a consequence of this analysis, the adaptive relaxation method and edge discontinuity treatment are then described with the automatic control of iterations explained in Sect. 3. Numerical tests are given in Sect. 4 and conclusions are drawn in Sect. 5.

2.The Fourth-Order PDE Model (YK Model)

In the past decade, many researchers proposed various fourth-order PDEs for image denoising. There are some benefits in using fourth-order PDEs. First, the fourth-order PDEs can suppress oscillation at high frequency more effectively than the second-order PDEs due to that the evolution of second order PDEs becomes weak in the high frequency areas. Second, for four-orde PDEs, there is of flexibility in employing

different functional behaviours in the formulation. In this section, an overview of the YK model is given and the shortcomings of this model are analysed and discussed.

2.1 An Overview of the YK Model

In 2000, You and Kaveh [11] proposed a time-dependent fourth-order PDE for image noise removal which is given by

$$\begin{cases} \dfrac{\partial u}{\partial t} = -\nabla^2[c(\| \nabla^2 u \|)\nabla^2 u], \ (x,y) \in \Omega, \ t > 0 \\ u(x,y,0) = u_0(x,y), \ (x,y) \\ \dfrac{\partial u}{\partial n} = \dfrac{\partial}{\partial n}(\nabla^2 u) = 0, \ (x,y) \in \partial\Omega \end{cases} . \tag{1}$$

where $u(x,y,t)$ is the grey-level function at scale t and u_0 is a noisy image. Ω is the image domain, $\partial\Omega$ is the boundary of Ω and n is the unit vector orthogonal to the boundary. In this model, You and Kaveh adopted the coefficient $c(\cdot)$ used in the anisotropic diffusion model, i.e.,

$$c(s^2) = \left(1 + \frac{s^2}{K^2}\right)^{-1}, \tag{2}$$

where K is a constant dependent on the image.

The YK model uses a piecewise planar image to approximate an original pure image. From the aspect of human visualization, a piecewise planar image looks more natural than the step image which second order PDEs employed to estimate the original image. This is the reason why it the YK model can prevent the "block effect" which is otherwise widely seen in all second order PDE models. In order to understand how this model works, the one-dimensional PDE of the form shown in Eqn (1) is considered [20], i.e.

$$\frac{\partial u}{\partial t} = -\frac{\partial^2}{\partial x^2}\left(c\left(\left(\frac{\partial^2 u}{\partial x^2}\right)^2\right)\frac{\partial^2 u}{\partial x^2}\right). \tag{3}$$

Expanding the right-hand side of Eqn (3) leads to

$$\frac{\partial u}{\partial t} = -\left(2\left(\frac{\partial^3 u}{\partial x^3}\right)^2 \Phi_1\left(\left(\frac{\partial^2 u}{\partial x^2}\right)^2\right)\right)\frac{\partial^2 u}{\partial x^2} - \Phi_2\left(\left(\frac{\partial^2 u}{\partial x^2}\right)^2\right)\frac{\partial^4 u}{\partial x^4}. \tag{4}$$

where $\Phi_1(s^2) = 2c''(s^2)s^2 + 3c'(s^2)$ and $\Phi_2(s^2) = 2c'(s^2)s^2 + c(s^2)$. The local behaviour of Eqn (4) depends on the signs of Φ_1 and Φ_2. If $\Phi_1\left(\left(\frac{\partial^2 u}{\partial x^2}\right)^2\right) < 0$, it leads to the second order part forward diffusion, otherwise to a second order part backward diffusion. Likewise, if $\Phi_2\left(\left(\frac{\partial^2 u}{\partial x^2}\right)^2\right) > 0$, Eqn(4) performs the fourth-order forward diffusion, whereas $\Phi_2\left(\left(\frac{\partial^2 u}{\partial x^2}\right)^2\right) < 0$ ensures a fourth order backward diffusion.

Nevertheless, this model tends to leave the resulting images with isolated white and black speckles (See Fig. 1(b)). These speckles can be featured as the pixels which are either much lighter or much darker than their neighbouring pixels. You and Kaveh thought that the piecewise planar images have weaker masking capability than step images used in anisotropic diffusion [11]. More specific reasons of this problem are explained in [21]. To understand the reasons, a control process is applied on the black point (denoted as the central point) in Fig. 1(c) and its four neighbouring points.

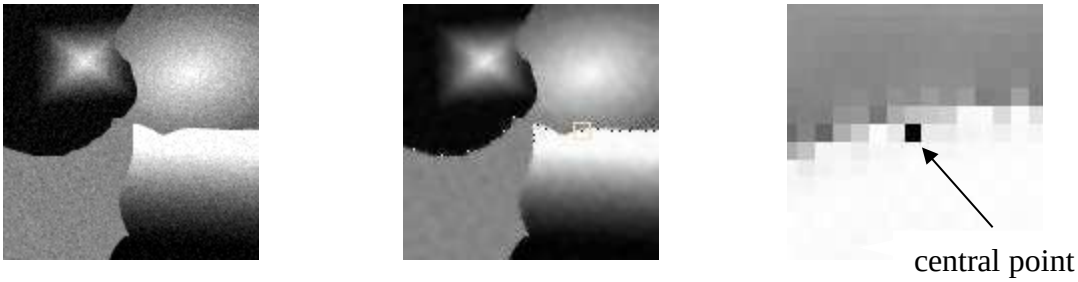

(a) (b) (c)

Fig. 1 Isolated speckles in the denoised image obtained by YK model. (a) is the image with 10 dB Gaussian noise, (b) is the denoised image by the YK model and (c) is the Zoom-in of the square pixel shown in (b)

The changes of values of intensity at the central point above its four neighbouring points are shown in Fig. 2.

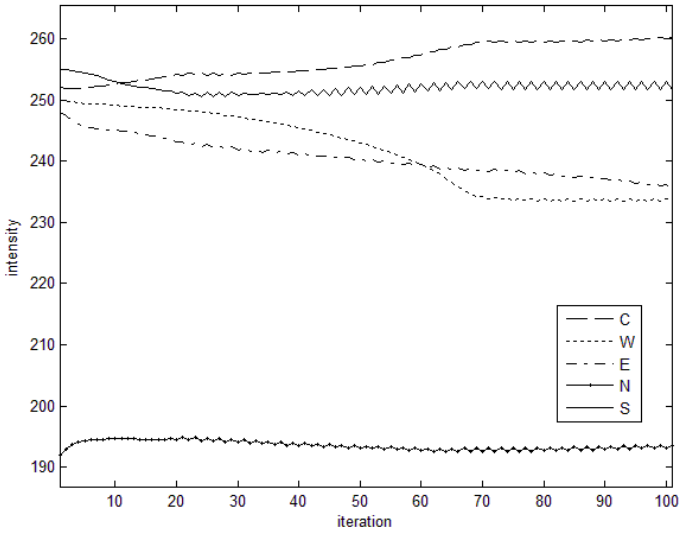

Fig. 2 Change of intensity around isolated speckles. C, W, E, N, S denotes the central point and its four neighbouring points in Fig. 1(c).

Fig. 2 exhibits the fact that the intensity of the central point increases markedly whereas the intensity of the neighbouring points either decreases (points on the north and south of the central point) or fluctuates slightly. As a result, the difference in pixel intensity between the central point and its neighbouring points becomes bigger and bigger as the iteration goes on. On the other hand, from Fig. 2, it should be noted that the value of the intensity of the central point exceeds 255 which is the extreme value when storing an image. Thus, if the image is stored at this current iteration, the point would be cast to black point. The same case applies to the white points. From the above discussion, the reasons of isolated speckles can be summarised as

1) The intensity of some points is changing more quickly than their neighbouring points or they change in different ways, i.e., the intensity of the central point increases, whereas intensities of its neighbouring points decrease.
2) The intensities of some points are not in the range [0, 255] for a grey-value image of an image used in computer vision.

2.2 Implementation of the YK model

Before introducing the relaxation method into the iterative processing of the YK model, the discretisation of the YK model is simply decribed below.

Firstly, Eqn (1) can be rewritten as:

$$\frac{\partial u}{\partial t} = -\nabla^2 g \,,$$

$$g = c(\nabla^2 u\,|)\nabla^2 u\,.$$

Suppose the size of image is $Ih \times Jh$, where h means the grid size of ~~discretization~~discretisation, Δt is the temporal step size. The discretisation process can be applied as following steps.

Step 1: Calculate $\nabla^2 u$ ~~,~~.

$$\nabla^2 u_{i,j}^n = u_{i+1,j}^n + u_{i-1,j}^n + u_{i,j+1}^n + u_{i,j-1}^n - 4u_{i,j}^n \quad i = 0,1,2,\cdots I,\ j = 0,1,2,\cdots J,$$

With the symmetric boundary conditions.

$$\begin{matrix} u_{-1,j}^n = u_{0,j}^n, u_{I+1,j}^n = u_{I,j}^n \\ u_{i,-1}^n = u_{i,0}^n, u_{i,J+1}^n = u_{i,J}^n \end{matrix}.$$

Step 2: Calculate function g.

$$g_{i,j}^n = c(\nabla^2 u_{i,j}^n)\nabla^2 u_{i,j}^n.$$

Step 3: Calculate $\nabla^2 g$.

$$\nabla^2 g_{i,j}^n = \frac{g_{i+1,j}^n + g_{i-1,j}^n + g_{i,j+1}^n + g_{i,j-1}^n - 4g_{i,j}^n}{h^2},\ i \quad 0,1,2\cdots I,\ j \quad 0,1,2,\cdots J,$$

with symmetric boundary conditions.

$$\begin{matrix} g_{-1,j}^n = g_{0,j}^n, g_{I+1,j}^n = g_{I,j}^n \\ g_{i,-1}^n = g_{i,0}^n, g_{i,J+1}^n = g_{i,J}^n \end{matrix}.$$

Step 4: Calculate the iterative equation.

$$u_{i,j}^{n+1} = u_{i,j}^n - \Delta t \nabla^2 g_{i,j}^n.$$

Step 5: Go to Step 1 if the pre-assigned number of iteration is not completed.

3. An improved Fourth-Order PDE Denoising Method

3.1 An Adaptive Relaxation Method

Relaxation methods ~~are~~ were established in numerical schemes in many areas involving the solutions of simultaneous equations and systems of inequalities resulting from discretisation schemes. Relaxation can be applied to any systems of linear or nonlinear equations to speed up an estimation to an exact solution. The basic

idea is to guess a solution and obtain an improved approximation such that the error is reduced until it is less than some specified tolerance [34].

In general, relaxation methods are used to control the variation of approximate solutions between consecutive iterations. As mentioned in Sect. 2, speckles appear in the numerical solution process because pixel intensities of some points are changing too fast. Therefore, it is reasonable to employ a relaxation method in the process of denoising when using the YK model. In this paper, an adaptive relaxation method is proposed to relieve the generation of speckles in the YK model. Since the isolated speckles are local extreme values, such as in a 3~~-by~~x~~-~~3 neighbourhood, an isolated-point-detection scheme which is developed in Sec. 3.2 is added to the algorithm when relaxation method is applied. The adaptive relaxation method can be explained as follows.

Suppose u^n is the iterative solution of the discrete approximation of Eqn (1) at time $t = n\Delta t$, where Δt means the time step size of the iteration. For a point $p \in \Omega$, $u_{\max}$ and $u_{\min}$ are the maximum and minimum intensity values of a deleted neighbourhood of p (i.e. neighbourhood of p without p). Let $u_{globalmax}$ and $u_{globalmin}$ be the global maximum and minimum values of the image u. Then define $globalmax = 0.9 \cdot u_{globalmax}$ and $globalmin = 1.1 \cdot u_{globalmin}$. If $u_p^n \notin [u_{max}, u_{min}]$ or $u_p^n \notin [globalmin, globalmax]$, then one has

$$~~u~~u_p^n = (1 \quad \lambda(~~n~~n))u_p^{n-1} \quad \lambda(n)u_p^n, \tag{5}$$

~~Here~~ here $\lambda : [0, +\infty] \mapsto [0,1]$ is a monotonically non-decreasing function with regard to the number of iteration~~s~~s, e.g., $\lambda(n) = 1 - e^{(-0.01n)}$. If the intensity of the central point in a 3~~-by~~x~~-~~3 window changes significantly, it can be restrained by using Eqn (5) to avoid too rapid a variation, leading to divergence of the iterative scheme. The result obtained by the adaptive relaxation method for Fig. 1(a) is shown in Fig. 3(a). It can be seen from the result that the intensities along the edges are not continuous. This may be due to the local character of the relaxation method. Therefore, a discontinuity treatment for edges is needed which is proposed in Sect. 3.2. The aim of this treatment is to make the edges look more natural in an image following the denoising procedure.

(a) (b)

Fig. 3 Results of using relaxation methods. (a) and (b) are the denoised images by the YK model without and with discontinunity treatment, respectively

3.2 The Discontinuity Treatment

To handle the discontinuity on ~~the~~ edges, the first step is to detect the discontinous pixel points along the edges. In the literature, the mask below is used to recognise the discontinuous points around the edges[23],

$$\begin{bmatrix} w_1 & w_2 & w_3 \\ w_4 & w_5 & w_6 \\ w_7 & w_8 & w_9 \end{bmatrix},$$

The response, R, of the mask applied at any point in an image is given by

$$R = \sum_{i=1}^{9} w_i u_i \quad , \tag{6}$$

where u_i is the intensity of the pixel at position *i* in the mask above and w_i is the weighted coefficient of the mask. Detection of the discontinuous points on which the mask is centered occurs if

$$|R| \geq T \, . \tag{7}$$

Here *T* is a non-negative threshold. The underlying idea of this method is to make use of the intensity difference, which is determined by the threshold *T*, between an isolated point and its neighbouring points.

After detecting the discontinuous points on the edges, in order to restore better values of the pixels at such points, the types of edges where these points are located need to be examined. For simplicity, only four simple types of edges are to be taken into consideration, including horizontal edges, vertical edges, and inclined edges oriented at 45º and -45º directions. The corresponding masks are shown as below [23]:

$$\begin{bmatrix} -1 & -1 & -1 \\ 2 & 2 & 2 \\ -1 & -1 & -1 \end{bmatrix} \quad \begin{bmatrix} -1 & 2 & -1 \\ -1 & 2 & -1 \\ -1 & 2 & -1 \end{bmatrix} \quad \begin{bmatrix} -1 & -1 & 2 \\ -1 & 2 & -1 \\ 2 & -1 & -1 \end{bmatrix} \quad \begin{bmatrix} 2 & -1 & -1 \\ -1 & 2 & -1 \\ -1 & -1 & 2 \end{bmatrix}$$

(a) (b) (c) (d)

Fig. 4 Edge ~~detector~~ detective masks corresponding to the horizontal, vertical, 45° and -45° directions

Four different masks are proposed here to restore the discontinuous pixel points on edges defined in the above modes respectively (See Fig. 5). Here the weighted coefficients are chosen such that the central point takes the most weight and then the points along the edge which the central point locates at. Other points take the same but the least weight. For example, if a discontinuous pixel point is located on a horizontal edge, then the template to be used is as in Fig. 5(a). The result of using the relaxation method together with the discontinuity treatment is shown in Fig. 3(b).

$$\begin{bmatrix} 0.05 & 0.05 & 0.05 \\ 0.2 & 0.3 & 0.2 \\ 0.05 & 0.05 & 0.05 \end{bmatrix} \quad \begin{bmatrix} 0.05 & 0.2 & 0.05 \\ 0.05 & 0.3 & 0.05 \\ 0.05 & 0.2 & 0.05 \end{bmatrix} \quad \begin{bmatrix} 0.05 & 0.05 & 0.2 \\ 0.05 & 0.3 & 0.05 \\ 0.2 & 0.05 & 0.05 \end{bmatrix} \quad \begin{bmatrix} 0.2 & 0.05 & 0.05 \\ 0.05 & 0.3 & 0.05 \\ 0.05 & 0.05 & 0.2 \end{bmatrix}$$

(a) (b) (c) (d)

Fig. 5 Discontinuous point restored masks corresponding to the horizonal, vertical, 45° and -45° directions

3.3 A Control of Iteration

In numerical analysis, the L_2-norm is often used to control the convergence, that is [36],

$$\left\| u^n - u^{n-1} \right\|_{L_2} = \sqrt{\sum_{i,j \in \Omega} (u_{i,j}^n - u_{i,j}^{n-1})^2} < \varepsilon ,$$

where Ω is the problem domain and ε is the tolerance usually set as 10^{-4}. However, this norm is not usually employed in image processing. In the literature, most papers simply set the number of iterations as an input ([4], [11], [12], etc.), and some papers proposed different criteria according to their specific models [37], [38]). Therefore, it is sensible to find a certain quantity to control the number of iteration. As mentioned in Sect. 2, with the iteration proceeding, the asymptotic value of $\nabla^2 u$ lies close to zero, as $t \to \infty$, which means $\nabla^2 u$ could be used to terminate the iteration. In this paper, the average value of $\nabla^2 u$ over all pixels is proposed to control the iteration process.

$$\hat{I} = \frac{\sum_{i,j} |\nabla^2 u_{ij}|}{W \times H}. \tag{8}$$

In order to investigate the features of $\hat{I}$, the relationship between $\hat{I}$ and the number of iteration is studied using the YK model. Here the image in Fig. 1(a) and two other benchmarking images in Fig. 7 are used for testing.

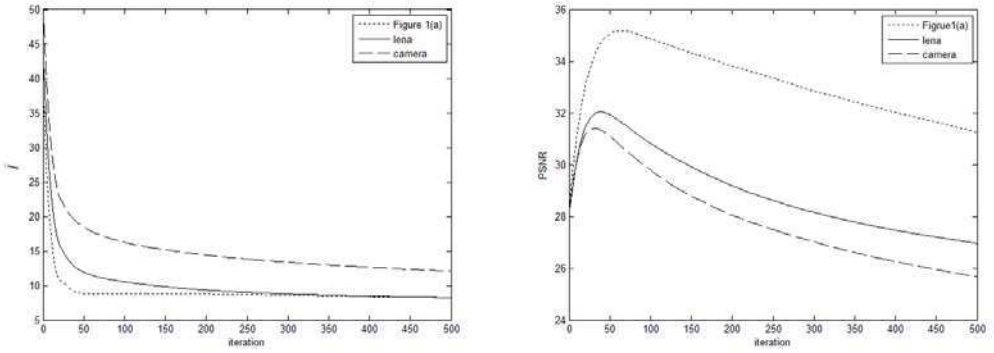

(a) (b)

Fig. 6 Profiles of $\hat{I}$ and PSNR with regard to the number of iteration

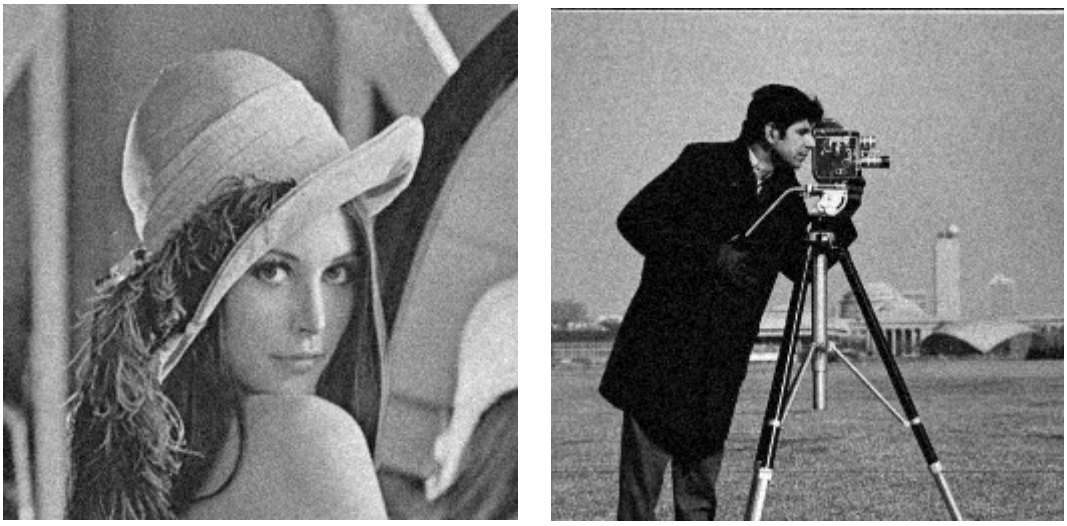

(a) (b)

Fig. 7 Two benchmarking images with 10dB Gaussian noise. (a) Lena, (b) Camera

Fig. 6(a) shows that after certain number of iterations, the value of $\hat{I}$ becomes constant. Furthermore, by comparing Fig. 6(a) and Fig. 6(b), it is easily obtained that when the values of PSNR reach their peak, values of $\hat{I}$ tend to become constant. Therefore, it is reasonable to assume that when the value of $\hat{I}$ is nearly constant, the value of PSNR is most likely to be high. Based on this analysis, the following condition is proposed to control the iteration:

$$\left|\hat{I}^{n} - I^{n-1}\right| < \varepsilon . \tag{9}$$

Here ε is a tolerance which can be chosen for different applications.

4. Numerical Tests

4.1 Algorithm Description

Suppose the size of image is $Ih \times Jh$, where h means the grid size of discretization, Δt is the temporal step size. Standard finite difference notation for the discretisation is used in the description of the algorithm. The improved algorithm can be described as below:

1. Initial noisy image u^0, Set $n := 0$ and $\hat{I}^0 := 0$;

2. Calculate $\nabla^2 u^n$ and $\nabla^2 g = \nabla\left(c(\nabla u^n)\nabla u^n\right)$;

3. Calculate $u^{n+1} = u^n - \Delta t \nabla^2 g^n$;

4. If $u^n \notin \left[u_{\max}, u_{\min}\right]$ or $u^n \notin \left[globalmax, globalmin\right]$, $u^{n+1} = \left(1 - \lambda(n)\right)u^{n+1} + \lambda(n)u^n$;

5.calculate $\hat{I}^{n+1}$, If $\left|\hat{I}^{n+1} - I^n\right| \geq \varepsilon$, goto 6, else goto 7;

6. update $n := n+1$, goto 2;

7. Use the discontinuity treatment in Sect. 3.2 to restore the discontinuous points on the edges.

Remarks:

a: The discretised form of the Laplacian is computed as below:

$$\nabla^2 u_{i,j}^n = \frac{u_{i+1,j}^n + u_{i-1,j}^n + u_{i,j+1}^n + u_{i,j-1}^n - 4u_{i,j}^n}{h^2};$$

b: The symmetric condition is used along the boundary:

$$u_{-1,j}^n = u_{0,j}^n, u_{I+1,j}^n = u_{I,j}^n \quad j = 0,1,2,\cdots J.$$
$$u_{i,-1}^n = u_{i,0}^n, u_{i,J+1}^n = u_{i,J}^n \quad i = 0,1,2,\cdots I.$$

c: $u_{\max}$ *and* $u_{\min}$ are the local maximum and minimum values of a 3 by 3 neighbourhood of the current point;

d: *globalmax* and *globalmin* are the 90% of global maximum and minimum values in the current image;

e: $\lambda(n) = 1 - e^{(-0.01n)}$;

f: In Eqn (9), $\varepsilon = 10^{-3}$;

g: the mask used in Eqn (6) is

$$\begin{bmatrix} -1 & -1 & -1 \\ -1 & 8 & -1 \\ -1 & -1 & -1 \end{bmatrix}$$

h: Eqn (7) is modified as $|R| > global\_max$ or $|R| < global\_min$ and the values of *globalmax* and *globalmin* are the same as those in Remark *c*;

4.2 Numerical Experiments

In this experiment, the fourth-order PDE model for image denoising proposed by You and Kaveh (YK model) and the fourth-order PDE model with the relaxation method and the discontinuity treatment (AYK) are tested.

To make the results more obvious, several images with different simple edges are designed to test the performance of the AYK model when coming across the discontinuity at the edges.

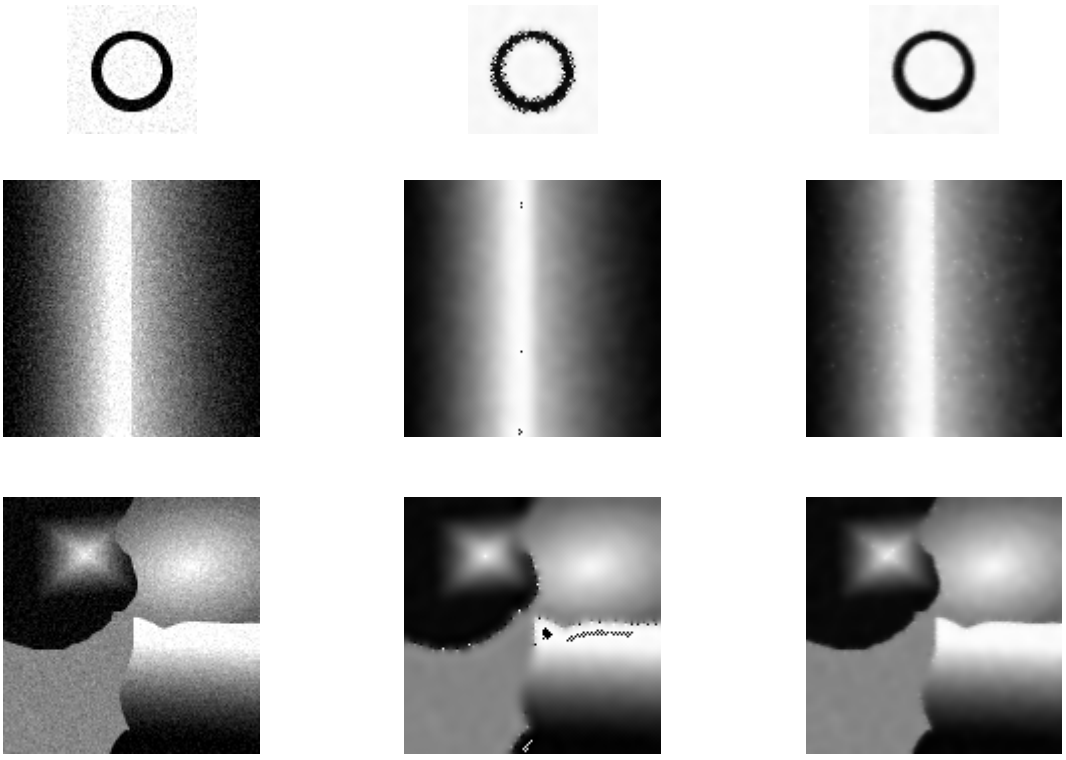

(a) (b (c)

Fig. 8 A set of experiments by using the YK model and the proposed model. Column (a): Three test images with 10 dB Gaussian noise, Column (b): The corresponding denoised images by the YK model, Column (c): The corresponding denoised images by ~~the proposed~~AYK model.

From Fig. 8, it can be seen that no matter what kind of edges are present, the YK model cannot handle them well and the isolated speckles exist both in the flat area near the edges and on the edges. Especially for the circle image, after ~~processing~~ processed by the YK model, although the noise in the flat area is removed, there are many speckles generated around the circles. However, the resulting images in Fig. 8(c) shows that the AYK model not only removes noise efficiently, but also succeeds in avoiding the speckles and preserves edges better than the YK model.

In order to verify the validity of the proposed model, experiments including two groups of 1-D signals and 2-D images shown in Fig. 7 are conducted in the following section. The WYK model proposed in [29] is used for comparison.

For the 1-D signal demonstration, in order to compare the similarity between the denoised signal and the original signal quantitatively, the L_1-norm defined as below is employed in this paper,

$$Error = \int |f(x) - g(x)| dx \,,$$

where *f(x)* and *g(x)* means the original and denoised signals. The two groups of 1-D signals experiments are shown in Fig. 9 with the corresponding error measurement in Table 1.

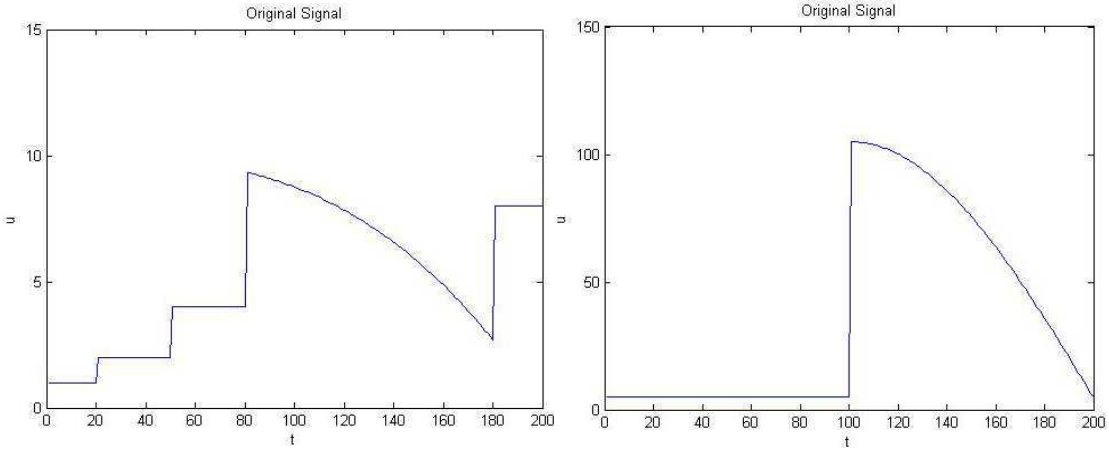

(a)

(b)

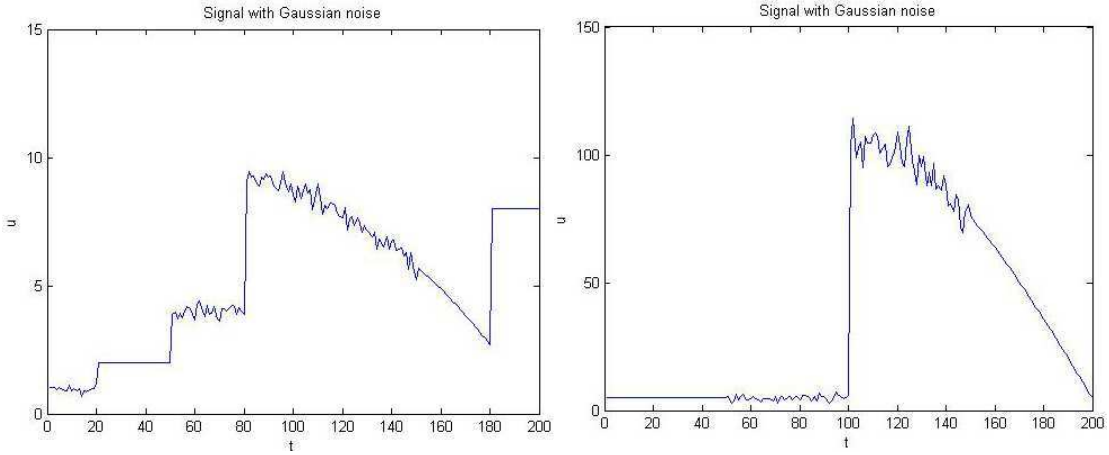

(c)

(d)

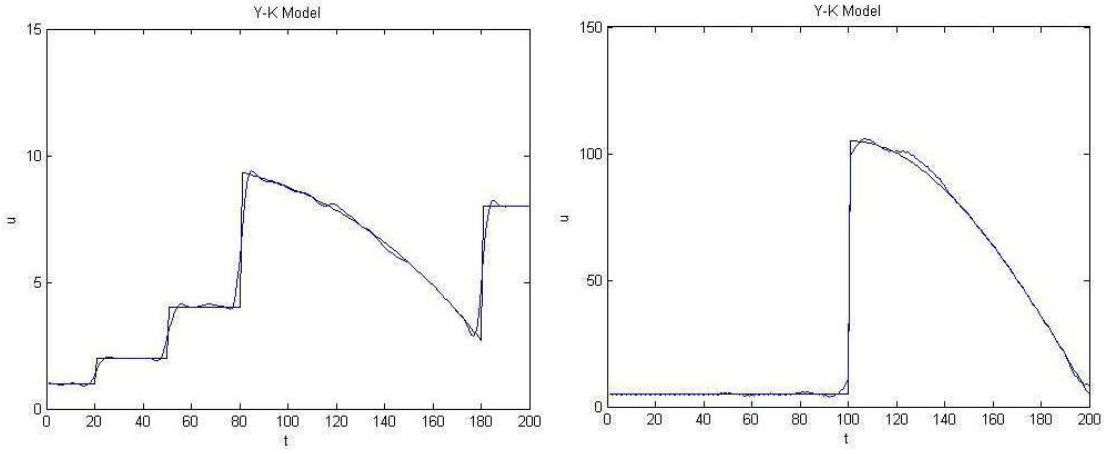

(e)

(f)

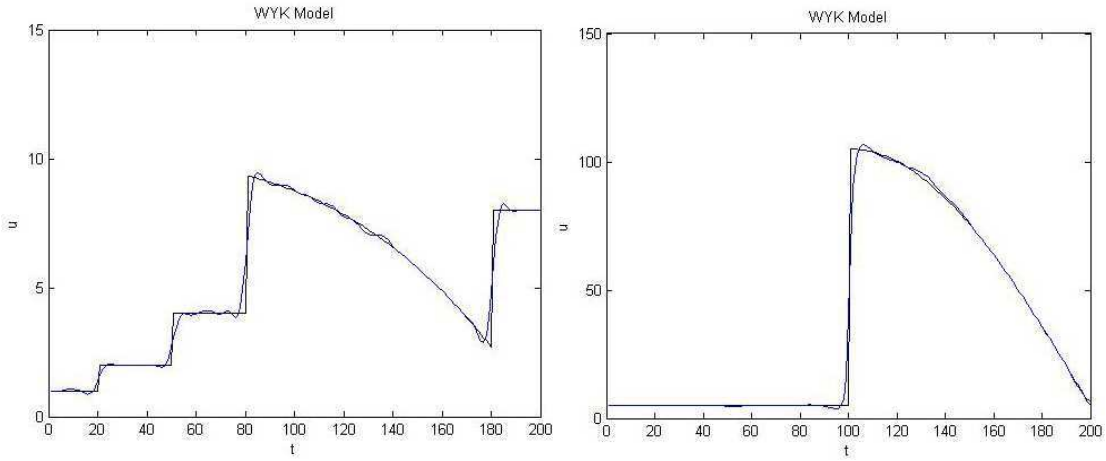

(g) (h)

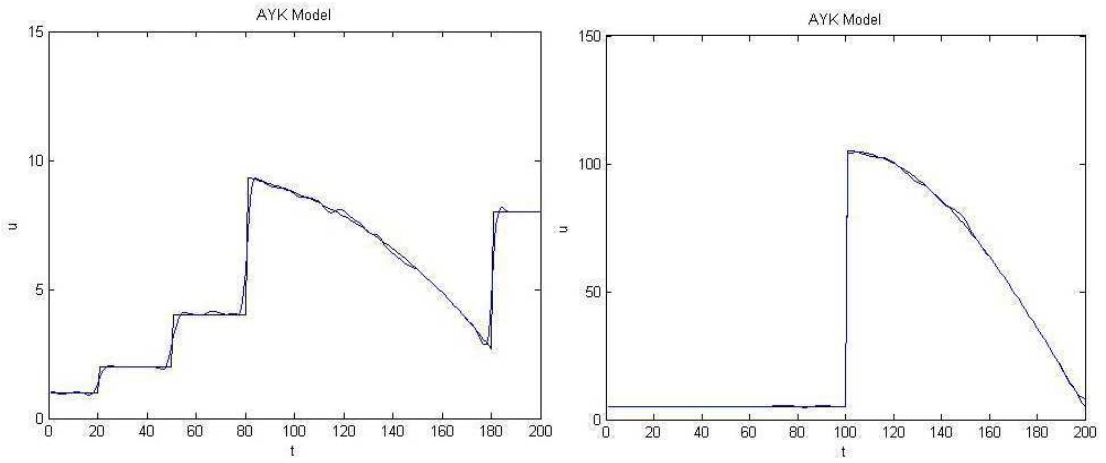

(i) (j)

Fig. 9 1-D signal demonstration. The first column includes~~are~~ the original signal a, its corresponding noisy signal, the denoised signals by the YK model, the WYK model, and the AYK model, respectively. The second column ~~are~~ is the original signal b and the denoised results.

From this demonstration, it can be seen that all three fourth order PDE models can remove the noise from the signal, although some details are lost, more or less. By comparing the results, one can observe that, for signal a, the performance of these three models are almost the same. For signal b, the AYK model provides the best result, ~~whether~~ whatever in the flat area ($t \in [0,50]$, small oscillation in the YK model) or in the noisy area ($t \in [51,100]$, small oscillation in the YK and WYK models). In such a case, the AYK model performs better than the YK and WYK models. The error measurement shown in Table 1~~.~~ can also draw the same conclusion.

Table 1 Error measurement for Fig. 9

Signal / *Error* / *Model*	*a*	*b*
Noisy signal	25.64	243.15
Y-K model	24.59	140.44
WYK model	23.22	134.35
AYK model	23.61	97.15

The 2-D image demonstration uses the two benchmarking images, Lena and Camera to test the performance amongst the three models mentioned above. The error measurement used for 2-D image experiments is PSNR which is defined as below.

$$PSNR = 10 \cdot \log_{10} \left(\frac{255 \times 255}{\frac{1}{W \times H} \sum_{i=1}^{W} \sum_{j=1}^{H} [I(i,j) - u(i,j)]^2} \right),$$

where W and H are the width and height of an image investigated, respectively. $I(i,j)$ and $u(i,j)$ are the grey values corresponding the original pure image and the restored image.

(a)

(b)

(c) (d)

(e) (f)

Fig. 10 Denoised results. (a) and (b) are the results by the YK model, (c) and (d) are the results by the WYK model, (e) and (f) are the results by the AYK model.

The value of the threshold K in three models above is chosen as 10 and the time step $\Delta t = 0.25$. As seen in Fig. 10, the AYK model can play a good role in removing noise and the isolated speckles produced by the YK model are diminished. From the results given by the Y-K model, one can see that although noise is removed, some isolated speckles are brought in. The WYK model, on one hand, performs noise removal and keeps more details than the Y-K model. On the other hand, it still leads to isolated speckles. However, it relieves this symptom to some extent. The AYK model not only removes noise from the image, but also avoids isolated speckles successfully. Comparing with the results given by the WYK model, it leads to more details lost. In

the following section more objective information is provided to compare the two algorithms.

Fig. 11 provides the PSNR comparison amongst three models, which shows that the WYK and AYK models present better PSNR values than Y-K model and in the long term, the AYK model degrades the image more slowly than the WYK and Y-K model.

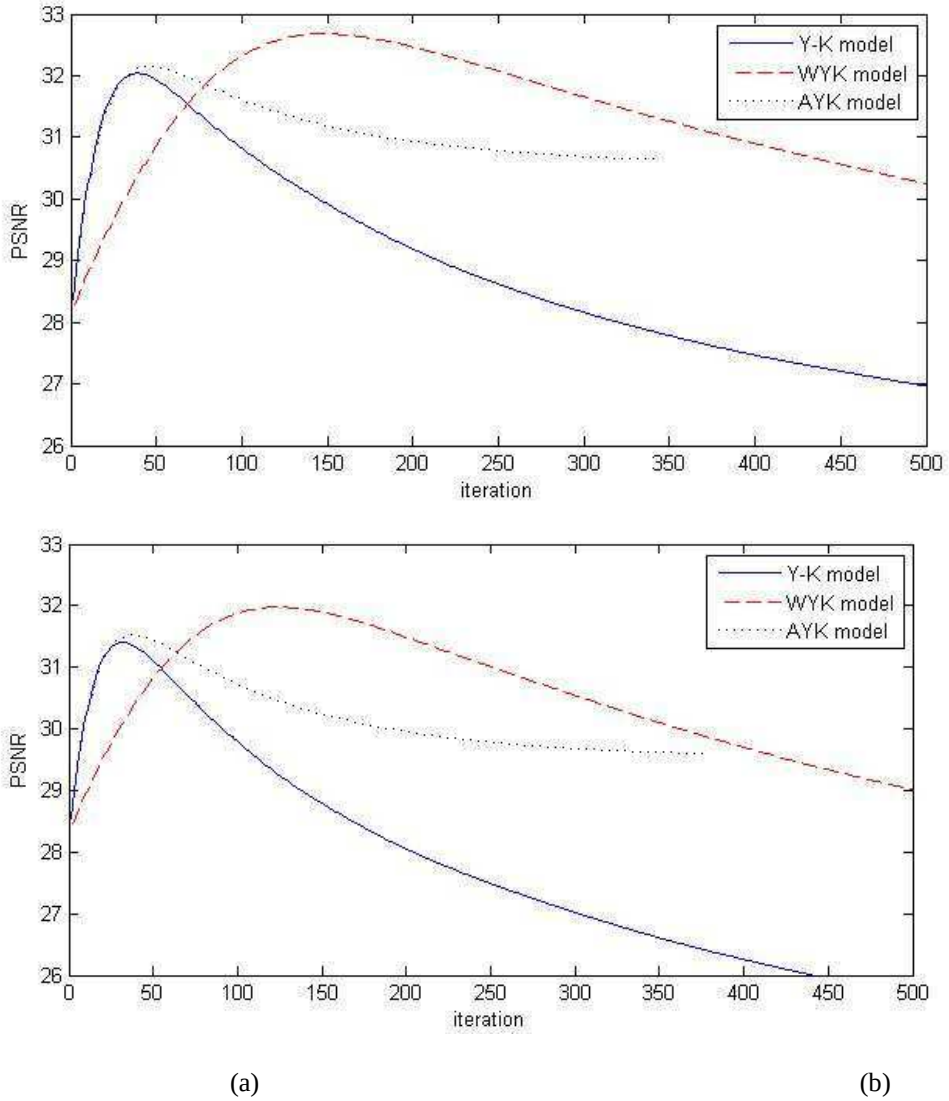

(a) (b)

Fig. 11 The variation of PSNR, (a) with the image Lena, (b) with the image Camera

From these two graphs, at the beginning of the process, the values of PSNR almost overlap since the value of λ is small at first. After that, the performance of the proposed method is much better than that of the YK model. The value of PSNR remains higher and also requires a fewer number of iterations to yield a higher value of PSNR.

~~Figure 7.6 shows the three models applied to the benchmark images, Lena and Camera.~~

5. Conclusion

In this paper, an adaptive relaxation method and a discontinuity treatment are proposed to improve the performance of the YK model. With such modifications, on one hand, not only the noise from an image may be removed more efficiently, but also it preserves the YK model's favourable properties, e.g, the reduction of staircasing effect presenting in the second order PDE models. On the other hand, the isolated speckles brought in by the YK model vanish. In addition, the proposed method can preserve more details of the original image and protect the edges well which is one of the main purposes of image denoising. Finally a stopping control of the iterative process is proposed to make the algorithm automatic, which may be generalised to other PDE models for image denoising.

References

1. Lee, J. S.: Digital Image Enhancement and Noise Filtering by Use of Local Statistics. IEEE Trans. Pattern Anal. Mach. Intell., **2**(2), 165-168 (1980)
2. Coifman R. R., Donoho D. L.: Translation-invariant De-noising. Wavelet and Statistics, Springer Lecture Notes in Statistics, **103**, 1995.
3. Chang S. G., Yu, B., Vetterli M.: Image Denoising via Lossy Compression and Wavelet Thresholding. Proc. IEEE Int. Conf. Image Process., **1**, 604-607 (1997)
4. Gilboa G., Sochen N.,Y. Zeevi Y.: Forward-and-Backward Diffusion Processes for Adaptive Image Enhancement and Denoising. IEEE Trans. Image Process., **11**(7), 689-703 (2002)
5. Buades A., Coll B., Morel J.-M.: A non-local algorithm for image denoising. Computer vision and Pattern Recognition, **2**, 60-65 (2005)
6. Roth S. and Black M. J.: Fields of Experts: A Framework for Learning Image Priors. Computer vision and Pattern Recognition, **2**, 860-867 (2005)
7. Buades A., Coll B., Morel J. M.: Nonlocal Image and Movie Denoising. Int. J. Comput. Vis., 76(2), 123-139 (2008)
8. Rajan J., Kannan K., Kaimal M. R.: An Improved Hybrid Model for Molecular Image Denoising. J. Math. Imaging Vis., **31**(1), 73-79 (2008)
9. Dabov K., Foi A., Katkovnik V., Egiazarian K.: Image Denoising by sparse 3D Transform-domain Collaborative filtering. IEEE Transactions on Image Processing, **16**(8), 2080-2095 (2007)

10. Burger H. C., Schuler C. J., Harmeling S.: Image Denoising: Can Plain Neural Networks Compete with BM3D? Computer Vision and Pattern Recognition, 2392-2399 (2012)
11. Koenderink J.: The Structure of Images. Biological Cybernetics, **50**(5), 363-370 (1984)
12. Perona P., Malik J.: Scale-space and Edge Detection Using Anisotropic Diffusion. IEEE Trans. Pattern Anal. Mach. Intell., **12**(7), 629-639 (1990)
13. Rudin L., Osher S., Fatemi E.: Nonlinear Total Variation Based Noise Removal Algorithms. Physica D, **60**(1-4), 259-268 (1992)
14. Rudin L. I., Osher S.: Total Variation Based Image Restoration with Free Local Constraints. 1st IEEE Int. Conf. Image Process., **1**, 31-35 (1994)
15. Guidotti P.: A Backward-forward Regularisation of the Perona-Malik Equation. J. of Dierential Equation, **252**(4), 3226-3244 (2012)
16. You Y.-L., Xu W., Tannenbaum A., Kaveh M.: Behavioral Analysis of Anisotropic Diffusion in Image Processing. IEEE Trans. Image Process., **5**(11), 1539-1553 (1996)
17. You Y.-L., Kaveh M.: Fourth-order Partial Differential Equations for Noise Removal. IEEE Trans. Image Process., **9**(10), 1723-1730 (2000)
18. Lysaker M., Lundervold A., Tai X. C.: Noise Removal Using Fourth-order Partial Differential Equation with Applications to Medical Magnetic Resonance Images in Space and Time. IEEE Trans. Image Process., **12**(12), 1579-1590 (2003)
19. Luminita A.V., Osher. S.: Image Denoising and Decomposition with Total Variation Minimization and Oscillatory Functions. J. Math. Imaging Vis., 2**0**(1-2), 7-18 (2004)
20. Lysaker M., Tai X. C.: Iterative Image Restoration Combining Total Variation Minimization and a Second-Order Functional. Int. J. Comput. Vis., **66**(1), 1-18 (2006)
21. Li F., Shen C., Fan J., Shen C.: Image Restoration Combining a Total Variational Filter and a Fourth-order Filter. J. Vis. Commun. Image Represent., **18**(4), 322-330 (2007)
22. Holm R.: Image Inpainting Using Nonlinear Partial Differential Equations. Thesis in Applied Mathematics, University of Bergen. http://www.uib.no/People/nmaxt/thesis/randi.pdf (2005). Accessed 07 February 2011
23. Yi D., Lee S.: Fourth-order Partial Differential Equations for Image Enhancement. Appl. Math. Comput., **175**(1), 430-440 (2006)
24. Chan T. F., Esedoglu S., Park F.: A Fourth Order Dual Method for Staircase Reduction in Texture Extraction and Image Restoration Problems. UCLA CAM Report 05-28 (2005)
25. Bai, J., Feng X.: Fractional-Order Anisotropic Diffusion for Image Denoising. IEEE Transactions on Image Processing, **16**(10), 2492-2502 (2007)
26. Hajiaboli M.R.: An Anisotropic Fourth-Order Partial Differential Equation for Noise Removal. Int J Comput Vis, DOI 10.1007/s11263-010-0330-1 (2009)
27. Guidotti P., Longo K.: Two Enhanced Fourth Order Diffusion Models for Image Denoising. Journal of Mathematical Imaging and Vision, **40**(2), 188-198 (2011)
28. Wang Y., Xue H.: Applying Fourth-Order Partial Differential Equations and Contrast Enhancement to Fluorescence Microscopic Image Denoising. Knowledge Discovery and Data Mining Advances in Intelligient and Soft Computing, **135**, 123-128 (2012)

29. Liu X. Y., Lai C. H., Pericleous K. A., Wang M. Q.: On a Modified Diffusion Model for Noise Removal. Journal of Algorithms and Computational Technology, **6**(1) 35-58 (2012)
30. Chan T., Marquina A, Mulet P.: High-order Total variation-based Image Restoration. SIAM J. Sci. Comput., **22**(2), 503-516 (2000)
31. Didas S., Weickert J.: Higher Order Variational Methods for Noise Removal in Signals and Images. Diploma thesis, Department of Mathematics, Saarland University. http://www.mia.uni-saarland.de/didas/pub/diplom.pdf (2004). Accessed 07 February 2011
32. Didas S., Weickert J., Burgeth B.: Stability and Local Feature Enhancement of Higher Order Nonlinear Diffusion Filtering. Pattern Recognit., **3663**, 451-458 (2005)
33. Lü L., Wang M., Lai C. H.: Image Denoise by Fourth-order PDE Based on the Changes of Laplaician. J. Algorithms Comput. Technol., **2**(1), 99-110 (2008)
34. Glowinski R.: Numerical Methods for Nonlinear Variational Problems. Springer (1984)
35. Gonzelaz R. C., Woods R. E.: Digital Image Processing (2nd Edition). Addison-Wesley Longman Publishing co., Inc., Boston (1992)
36. Press W. H., Teukolsky S. A., Vetterling W. T., Flannery B. P.: Numerical Recipes: The Art of Scientific Computing (3rd Edition). Cambridge University Press, Cambridge, UK (2007)
37. Lin Z. and Shi Q.: An Anisotropic Diffusion PDE for Noise Reduction and Thin Edge Preservation. Proc. 10th Int. Conf. Image Anal. Process., 102-107 (1999)
38. Joo K. and Kim S.: PDE-based Image Restoration: A Hybrid Model and Colour Image Denoising. IEEE Trans. Image Process., **15**(5), 1163-1170 (2006)